2017

A Method for Reflectance Index Wavelength Selection from Moisture-Controlled Soil and Crop Residue Samples

Ali Hamidisepehr
University of Kentucky, ali.hamidisepehr@gmail.com

Michael P. Sama
University of Kentucky, michael.sama@uky.edu

Aaron P. Turner
University of Kentucky, aaron.turner@uky.edu

Ole O. Wendroth
University of Kentucky, owendroth@uky.edu

A Method for Reflectance Index Wavelength Selection from Moisture-Controlled Soil and Crop Residue Samples

Notes/Citation Information
Published in *Transactions of the ASABE*, v. 60, issue 5, p. 1479-1487.

Digital Object Identifier (DOI)
https://doi.org/10.13031/trans.12172

A METHOD FOR REFLECTANCE INDEX WAVELENGTH SELECTION FROM MOISTURE-CONTROLLED SOIL AND CROP RESIDUE SAMPLES

A. Hamidisepehr, M. P. Sama, A. P. Turner, O. O. Wendroth

ABSTRACT. *Reflectance indices are a method for reducing the dimensionality of spectral measurements used to quantify material properties. Choosing the optimal wavelengths for developing an index based on a given material and property of interest is made difficult by the large number of wavelengths typically available to choose from and the lack of homogeneity when remotely sensing agricultural materials. This study aimed to determine the feasibility of using a low-cost method for sensing the moisture content of background materials in traditional crop remote sensing. Moisture-controlled soil and wheat stalk residue samples were measured at varying heights using a reflectance probe connected to visible and near-infrared spectrometers. A program was written that used reflectance data to determine the optimal pair of narrowband wavelengths to calculate a normalized difference water index (NDWI). Wavelengths were selected to maximize the slope of the linear index function (i.e., sensitivity to moisture) and either maximize the coefficient of determination (R^2) or minimize the root mean squared error (RMSE) of the index. Results showed that wavelengths centered near 1300 nm and 1500 nm, within the range of 400 to 1700 nm, produced the best index for individual samples. Probe height above samples and moisture content were examined for statistical significance using the selected wavelengths. The effect of moisture was significant for both bare soil and wheat stalks, but probe height was only significant for wheat stalk samples. The index, when applied to all samples, performed well for soil samples but poorly for wheat stalk samples. Index calculations from soil reflectance measurements were highly linear ($R^2 > 0.95$) and exhibited small variability between samples at a given moisture content, regardless of probe height. Index calculations from wheat stalk reflectance measurements were highly variable, which limited the usefulness of the index for this material. Based on these results, it is expected that crop residues, such as wheat stalks, will reduce the accuracy of remotely sensed soil surface moisture measurements.*

Keywords. *Near-infrared reflectance, Normalized difference water index, Remote sensing, Soil moisture, Spectroscopy.*

The development of irrigation and nutrient management practices for food production has resulted in substantial increases in crop yield, accounting for over 80% of the gains in the global supply of wheat, rice, and corn since the 1960s (Cassman, 1999). While this development has limited the expansion of agricultural land, it has also resulted in a reduction in biodiversity (Cardinale et al., 2012) and placed a large burden on global water resources (Hatfield, 2015). Nearly 23 million hectares of land were irrigated in the U.S. during 2012, accounting for 31% of total U.S. freshwater use (USDA, 2015). Many of the smart irrigation systems available for scheduling water application rely on either soil water holding capacity maps or low spatial resolution sub-soil sensor networks (Yule et al., 2008). Both methods may not be optimized, particularly in instances where the sensing technology is not spatially matched with the application technology. Increasing the spatial resolution of intensive management practices optimizes inputs and can reduce the overall level of inputs required to produce the same output (Raun et al., 2002).

Higher spatial resolution methods (10 m grid or smaller) for identifying water stress typically involve the use of remote sensing of a crop canopy using combinations of visible and near-infrared (Penuelas et al., 1997) or thermal infrared sensing (Carlson et al., 1981; Nemani and Running, 1989). Traditional deployments include satellite, conventional aircraft, and ground-based sensors but are limited in terms of cost, temporal resolution, and spatial resolution. Perhaps the most successful adoption of remote sensing technology in production agriculture has been the use of the normalized difference vegetation index (NDVI) to detect crop vigor, which is then correlated to a myriad of parameters in addition to water stress. These include vegetation cover (Carlson and Ripley, 1997), crop nitrogen status (Solari et al., 2008), crop yield (Benedetti and Rossini, 1993), and phenotype (Svensgaard et al., 2014). An alternative to NDVI is the normalized difference water index (NDWI), which typically uses longer wavelengths of light beyond the sensitivity of silicone-based photodiodes (Gao, 1996) and is potentially better suited to isolating water stress (Gu et al., 2007).

Submitted for review in November 2016 as manuscript number ITSC 12172; approved for publication by the Information, Technology, Sensors, & Control Systems Community of ASABE in June 2017.

The authors are **Ali Hamidisepehr, ASABE Member,** Graduate Student, **Michael P. Sama, ASABE Member,** Assistant Professor, and **Aaron P. Turner, ASABE Member,** Engineer Associate, Department of Biosystems and Agricultural Engineering, and **Ole O. Wendroth,** Professor, Department of Plant and Soil Sciences, University of Kentucky, Lexington, Kentucky. **Corresponding author:** Michael P. Sama, 119 C.E. Barnhart Building, University of Kentucky, Lexington, KY 40546; phone: 859-218-4325; e-mail: michael.sama@uky.edu.

  ISSN 2151-0032 https://doi.org/10.13031/trans.12172

Two challenges for remotely sensing crop water stress using traditional methods are the absorption of light due to atmospheric moisture and the contribution of soil reflectance to the overall vegetation reflectance spectra. Active ground-based sensors have been shown to overcome atmospheric limitations in nitrogen sensing by providing a light source (Raun et al., 2002; Mullen et al., 2003; Holland et al. 2004). The effect of soil type and conditions on canopy reflectance indices has also been addressed through calibrated indices, such as the soil adjusted vegetation index (SAVI) (Huete, 1998), or by removing the soil contribution from the reflectance spectra (Huang et al., 2009). In all the aforementioned applications, the crop was the visual target for indirectly measuring soil or crop parameters. However, there may still be useful information available from direct soil reflectance measurements. This work aims to study the reflectance spectra of bare soil and crop residue to determine if they can contribute to water stress detection. The ability to quantify soil moisture variability and its temporal dynamics over entire fields through direct soil observations using remote sensing will improve early detection of water stress before crop physiological or economic damage has occurred, and it will contribute to the identification of zones within a field where soil water is depleted faster than in other zones.

Objectives

The main objective of this study was to determine the feasibility of developing a low-cost reflectance sensor for remotely delineating soil moisture content from a ground-based or low-altitude UAS platform. Specific objectives include:

1. Collect visible and near-infrared spectral response from moisture-controlled soil and crop residue samples.
2. Identify the optimal wavelengths for a normalized index based on user-defined constraints.
3. Determine if the effect of sensor height above the sampled surface is statistically significant.

Material and Methods

Sample Preparation

In this study, samples with predetermined water contents were prepared from two materials: silt loam soil and wheat stalk residue. These materials were chosen because they represent potential background materials when observing row crops, such as corn or soybean, at early growth stages. Plastic containers of 120 mL volume with airtight removable lids were used to contain the moisture-controlled samples. The soil was air-dried, ground, and passed through a 2 mm sieve. The initial moisture content (wet basis) of the soil was determined gravimetrically by drying a sample in a convection oven at 105°C for over 24 h and measuring the resulting reduction in mass. The stalks were dried in a similar manner as the soil samples to prevent decomposition. Seven moisture levels were chosen: air dry (for soil) or 0% (for stalks), 5%, 10%, 15%, 20%, 25%, and 30%. Each container was marked at a volume of 35 mL (for bare soil) and 120 mL (for stalks), filled to the mark, and lightly tapped to firm up the soil or stalks. The mass of soil or stalks inside each sample container was measured with the mass of the container removed and used to determine the required mass of water to reach the target moisture content. Water was added to each sample using a pipet with a volumetric precision of 0.01 mL, and the final mass was recorded. The lid of each container was then closed, and the samples equilibrated for several days to allow the water to distribute through the sample. Three replications were prepared for each moisture level to minimize the effect of sample preparation error on statistical analysis. In total, 21 soil samples and 21 stalk samples were prepared.

Instrumentation Hardware

Reflectance was measured using visible and near-infrared spectrometers (HR400-7-VIS-NIR, NIRQuest512, Ocean Optics, Dunedin, Fla.) with a tungsten-halogen light source (HL-2000-HP-FHSA, Ocean Optics). A fiber optic reflectance probe (QR200-12-MIXED, Ocean Optics) was used to transmit source light to the sample and reflected light to the spectrometers. The reflectance probe consisted of twelve 200 μm diameter transmission fibers spaced concentrically around two 200 μm diameter reflectance fibers and was 2 m in length. The spectrometers were calibrated to 0% and 100% reflectance by blocking the light source for the background measurement and by using a Spectralon calibration target (WS-1-SL, Ocean Optics) for the reference measurement, respectively. The effective spectral range was 400 to 1700 nm with an overlap at 900 nm between the two spectrometers.

A consistent method was needed to position the reflectance probe above each sample to minimize bias and reduce variability due to probe height. A reflectance test fixture (fig. 1) was designed and fabricated to consistently position the spectrometer reflectance probe above the sample surface. The fixture consisted of three main components that were 3D

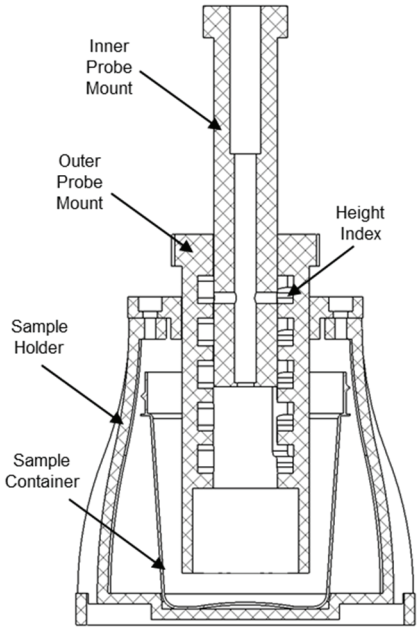

Figure 1. Cross-section view of the reflectance test fixture used to position the spectrometer probe above a soil or wheat stalk sample.

Table 1. Reflectance probe heights and resulting sampling diameters and sampling areas.

Height	Probe Height (cm)	Sampling Diameter (cm)	Sampling Area (cm^2)
H1	0.64	0.28	0.06
H2	1.92	0.84	0.55
H3	3.20	1.40	1.54
H4	4.48	1.96	3.02
H5	5.76	2.52	4.99

printed from black ABS plastic: a sample holder for centering the sample container underneath the probe, an outer probe mount that rested directly on top of the sample surface, and an inner probe mount for setting the height of the probe above the sample surface. The inner probe mount had stainless-steel dowel pins pressed into the sidewall that slid down guides in the outer probe mount. The height of the probe was set by rotating the inner probe mount inside the outer probe mount at one of five height index points. The probe heights were evenly spaced from 0.64 to 5.76 cm in increments of 1.28 cm. The 24.8° field-of-view (FOV) of the reflectance probe resulted in a sampling area of approximately 0.06 to 5 cm^2. The sampling diameters and areas for all heights are shown in table 1. The maximum height was selected based on the reflectance probe FOV and the sample size to limit the sidewalls of the outer probe mount from affecting the reflectance measurement.

Data Collection

OceanView software (ver. 1.4.1, Ocean Optics, Dunedin, Fla.) was used to configure the spectrometers and record the reflectance response. A graphical program was written that calculated the reflectance from each spectrometer, combined the two results into a single array, and graphed the results in real-time. The system was calibrated every time the height of the probe was changed and whenever the spectrometers and light source were powered on. The software was configured to record three measurements per sample. Given that there were three samples for each moisture content, three replications for each sample, and three measurements for each replication, there were 27 total reflectance responses for every combination of moisture content and height. This replication structure was intended to reduce the influence of variability in sample preparation, reflectance probe position, and sensor noise on the resulting index calculation.

Reflection measurements were normalized between 0 and 1 (0% and 100%) by subtracting the background measurement intensity from the raw measurement intensity and reference target measurement intensity and taking the ratio of the resulting differences (eq. 1):

$$R_\lambda = \frac{M_\lambda - C_\lambda^0}{C_\lambda^1 - C_\lambda^0} \quad (1)$$

where

R = normalized reflectance measurement from a sample (%)

M = raw measurement intensity from a sample (A/D counts)

C^0 = background measurement intensity with the light source obstructed (A/D counts)

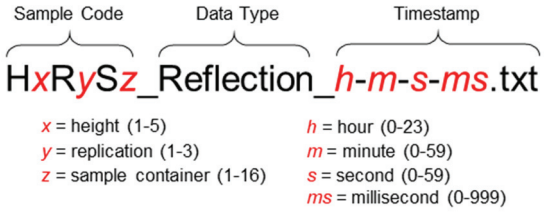

Figure 2. Filename format for output text files of the spectrometers. Fixed values are shown in black; variables are shown in red italics.

C^1 = reference target measurement intensity (A/D counts)

λ = specific wavelength (nm).

Each reflectance measurement was stored in a tab-delimited text file containing the spectral response along with the spectrometer settings. A filename format was used to label each text file to facilitate post-processing. Filenames included a sample code for identifying sensor height, replication, and sample container; a string corresponding to the data type within OceanView; and a local timestamp (fig. 2). A MATLAB script (R2015b, The Mathworks, Natick, Mass.) was written to access all text files from a single folder and categorize them using the filename sample code. The script stored data as columns in a single Excel spreadsheet with the corresponding sample codes as headers in the first row of each column.

Data Analysis

A second MATLAB script was written to perform data analysis. The script read in the entire dataset, calculated normalized indices for all pairs of wavelengths, and identified the "best" pair based on user-defined criteria. The normalized index was composed of two distinct narrowband ranges identified by their center wavelengths and obtained for every possible pair in ascending order over the 400 to 1700 nm range (eq. 2):

$$I_{\lambda 1,\lambda 2} = \frac{R_{\lambda 1} - R_{\lambda 2}}{R_{\lambda 1} + R_{\lambda 2}} \quad (2)$$

where

$I_{\lambda 1,\lambda 2}$ = normalized index for wavelengths centered at $\lambda 1$ and $\lambda 2$ (-1 to 1)

$R_{\lambda 1}$ and $R_{\lambda 2}$ = average reflectance at wavelengths centered at $\lambda 1$ and $\lambda 2$ (%)

$\lambda 1 > \lambda 2$ to reduce the number of computations by a factor of 2.

Selecting the "best" pair of wavelengths for calculating a reflectance index to predict moisture content implied several assumptions and required constraints to simplify the optimization process. It was assumed that the low-cost sensor would use either a silicon or indium-gallium-arsenide (InGaAs) photodetector coupled with narrow-band filters to detect specific wavelengths of visible and NIR light. For this study, the bandwidths were set to ±25 nm and were assumed to be uniformly distributed about a center wavelength. Preliminary reflectance index calculations using manually selected wavelengths revealed a linear relationship between sample moisture content and the normalized index. Moreov-

er, sensor height above the sample had little effect on index values. Therefore, a linear regression model was used to estimate moisture content based on the average normalized index measurement. Three optimization parameters were initially chosen: the coefficient of determination (R^2) of the linear regression between moisture content and the reflectance index, the root mean squared error (RMSE) between the actual and predicted moisture contents, and the slope of the linear regression, which represented sensitivity. The pair of wavelengths with the highest slope, the lowest RMSE, and the highest R^2 was considered the optimal solution by maximizing sensitivity and minimizing error. The optimization parameters were stored for each normalized index calculation and plotted in the form of slope versus R^2 and slope versus RMSE to determine if local optima or a global optimum existed.

A third script was written to determine the performance of the index for predicting moisture. The "best" wavelengths resulting from the previous step were used as inputs, and the normalized index for all samples was computed. A statistical analysis was conducted to determine if probe height above the sample was statistically significant. The experiment was set up with a factorial design using moisture content and height (7×5) with bare soil. The data were subjected to analysis of variance, and appropriate means separation was conducted using statistical software (JMP 12, SAS Institute, Cary, N.C.). The linear regression model from the average normalized index and the individual index values were used to determine a 95% prediction interval.

Results and Discussion

Spectrometer Calibration

The purpose of the calibration was to remove non-uniformity in the spectral response due to variability in the light source, optical fibers, and spectrometer detector with respect to wavelength. Figure 3 illustrates the raw intensity reference response from the spectrometers with the probe set to height H3 above the calibration target and the light source adjusted to maximize intensity without saturation at any wavelength of either spectrometer. The visible spectrometer always saturated before the NIR spectrometer and thus determined the intensity of the light source. Heights H4 and H5 used the full light source intensity and therefore did not use the full intensity range of either spectrometer. The other three heights produced similar responses that were scaled along the intensity axis. The intensity axis represents the raw analog-to-digital (A/D) converter results from the spectrometers' photodetectors. The visible spectrometer provided 14-bit resolution (0 to 16383) measurements, and the NIR spectrometer provided 15-bit resolution (0 to 32767) measurements.

Figure 4 illustrates the raw intensity background response from the spectrometers when the light source was blocked. The small variations across wavelengths were due to noise in the spectrometer detector. The NIR spectrometer had a large offset from zero as compared to the visible spectrometer, which was due to operating in high-gain mode. The high-gain mode was necessary to obtain a sufficient signal from the NIR spectrometer when using a single light source and reflectance probe.

Figure 5 shows the results of the calibration process in which non-uniformity was removed across all wavelengths when calculating the background reflectance and the reflectance from the reference target. Data from both spectrometers were spliced into a single dataset by removing data from the visible spectrometer past 900 nm and combining it with all data from the NIR spectrometer. Note that wavelengths below 500 nm still deviated from the desired 0% and 100% reflectance for the background and reference measurements, respectively. This was due to the low relative sensitivity of the visible spectrometer below this wavelength and indicated that more noise should be expected when using wavelengths in this range to calculate indices.

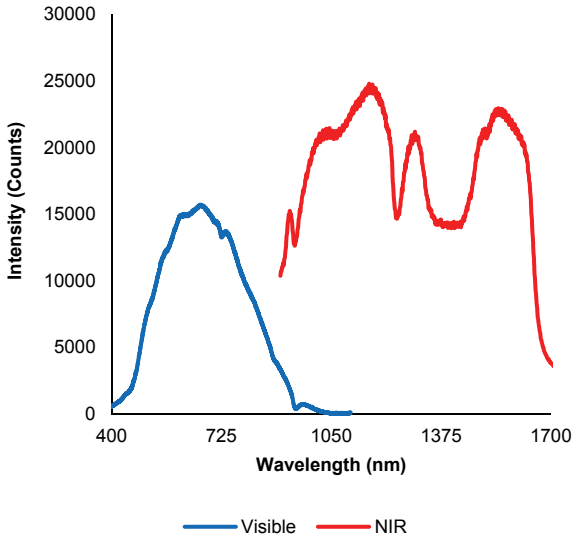

Figure 3. Intensity of reflected light versus wavelength for reference measurement at height H3 (3.2 cm).

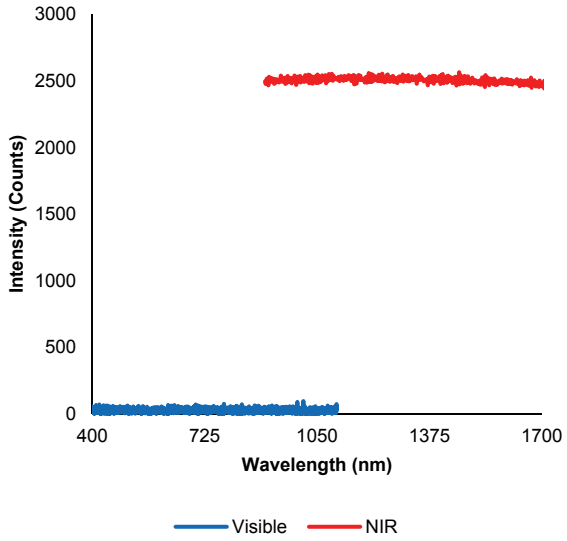

Figure 4. Intensity of reflected light versus wavelength for background measurement at height H3 (3.2 cm).

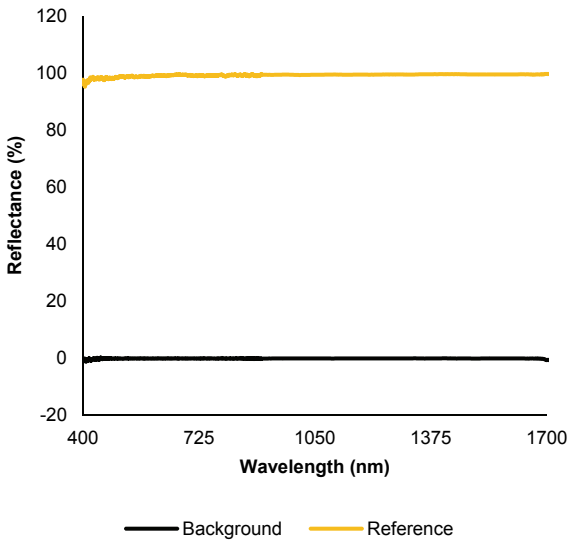

Figure 5. Calibrated and combined reflectance response for background and reference measurements at height H3 (3.2 cm).

Bare Soil

Figure 6 shows the reflectance for soil samples of varying moisture content versus wavelength. Each series is the average of all samples at a particular moisture content across all heights. The general spectral response of the soil samples was an increase in relative reflectance as wavelength increased. Drier samples typically reflected more light on average, but there were instances where the average reflectances across all wavelengths were not in order. For example, both the 25% and 30% moisture content samples measured at height H3 reflected more light than the 20% moisture content sample. This phenomenon was likely caused by small variations in the distance between the measured area and the spectrometer probe. Despite efforts to control the exact distance with the reflectance probe test fixture, uncontrolled variations in the soil surface shape (i.e., flat, convex, concave) likely had a substantial impact on the average reflectance. Given that the soil surface in the field would never be carefully controlled on the scale that was relevant to this experiment, no further adjustments to the sample were made. The non-ordered progression of average reflectance also illustrates why an index with two or more wavelengths is crucial for modeling the relationship between reflectance and moisture content. No single wavelength will produce a monotonic relationship with suitable sensitivity. However, it was observed that the relative dip in reflectance between 1400 and 1500 nm, when compared to other wavelengths for the same moisture content, exhibited a clear pattern. As moisture content increased, the relative reflectance within this range tended to decrease, while the rest of the spectral response followed a consistent profile.

The transition between the visible and near-infrared spectrometers at 900 nm produced a noticeable artifact in the relative reflectance measurement. Increasing the number of spectrometer calibration points between 0% and 100% reflectance might have mitigated this non-linearity, but a simpler solution was to ensure that wavelengths near this transition were not used when calculating an index.

As previously stated, the goal of the optimization process for selecting the "best" pair of wavelengths used to calculate a moisture content prediction index was to select the index that produced the largest slope while either maximizing the R^2 or minimizing the RMSE of the index function. Without knowing the relationship between the constraints, it was difficult to prioritize one constraint over the other. Rather than arbitrarily weighting each constraint, the resulting relationship between all pairs of wavelengths was plotted for both slope versus R^2 (fig. 7) and slope versus RMSE (fig. 8).

The resulting shapes revealed if local or global optima existed and illustrated an interesting trend between slope and either R^2 or RMSE. Points tended to follow deterministic paths as one wavelength was changed relative to another. The majority of slopes were negative, which was a result of the index equation in conjunction with the positive trend in

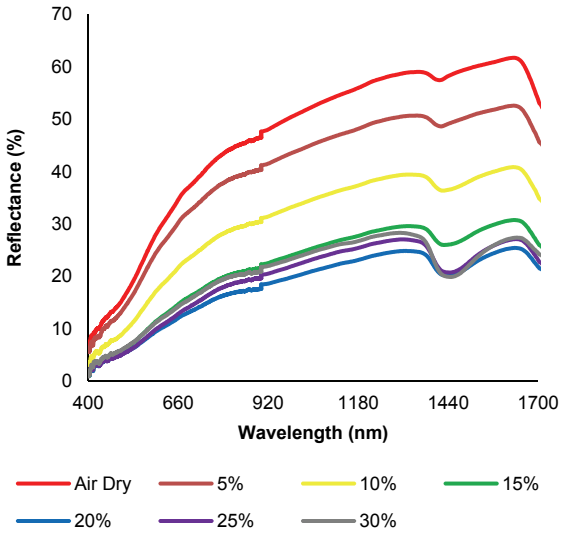

Figure 6. Average relative reflectance versus wavelength for varying nominal soil moisture contents of bare soil.

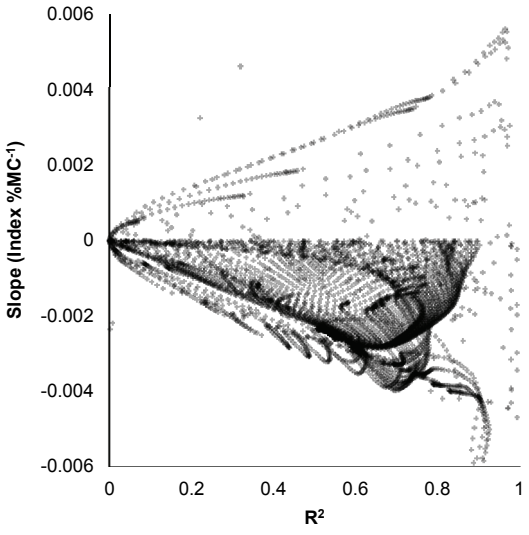

Figure 7. Slope of linear regression of reflectance and moisture content versus R^2 for bare soil.

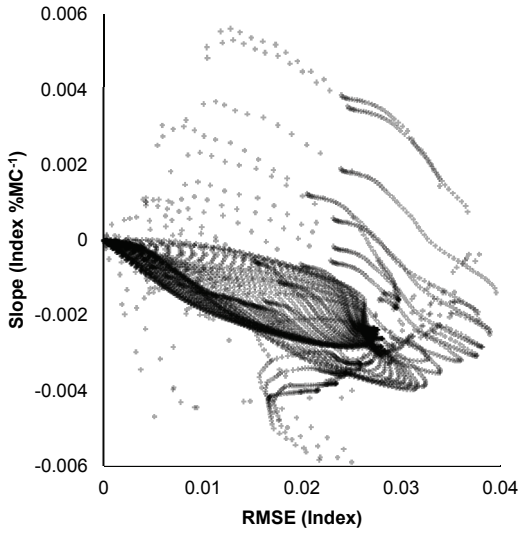

Figure 8. Slope of linear regression of reflectance and moisture content versus RMSE for bare soil.

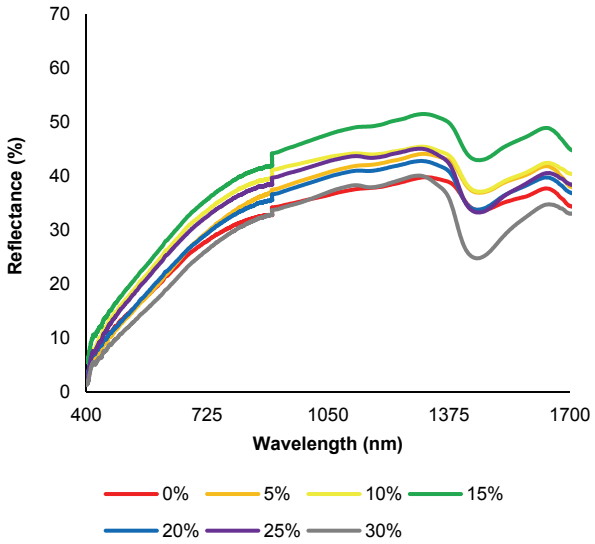

Figure 10. Average relative reflectance versus wavelength for varying nominal moisture of wheat stalk residue.

relative reflectance. Longer wavelengths generally exhibited a larger relative reflectance than shorter wavelengths, which produced a negative term in the index numerator. The sign could be fixed positive by always assigning the higher relative reflectance wavelength to λ_1. Figure 7 also reveals why R^2 and RMSE alone were not adequate for selecting the appropriate index wavelengths. As RMSE decreased, so did the slope of the index, which reduced the sensitivity of the index to moisture content. Similarly, the wavelengths that resulted in the highest R^2 also had a slope very close to zero.

There was no global optimum when using RMSE, but R^2 produced a grouping of indices where both the slope and R^2 were close to their respective maxima. The two wavelengths that produced this relationship were centered near 1300 nm and 1500 nm. When using RMSE, a peak occurred at a slope of approximately 0.0058 Index $\%MC^{-1}$ and an RMSE of 0.013. The corresponding wavelengths for this index were also centered near 1300 nm and 1500 nm.

The index values from 50 nm wide bands centered at 1300 nm and 1500 nm for all samples are shown in figure 9 along with the linear regression model and 95% prediction interval. Variability in the calculated index among samples at a given moisture content tended to increase as moisture content increased. Average index values varied from 0 to 0.15 for soil samples at 3.3% to 30% moisture content, respectively.

Wheat Stalk Residue

Wheat stalk residue produced a similar spectral response to bare soil, where the reflectance generally increased with respect to wavelength and a dip occurred between 1400 and 1600 nm (fig. 10). Both the discontinuities between the two spectrometers and the dip at the water absorption bands were more pronounced, while the average difference in reflec-

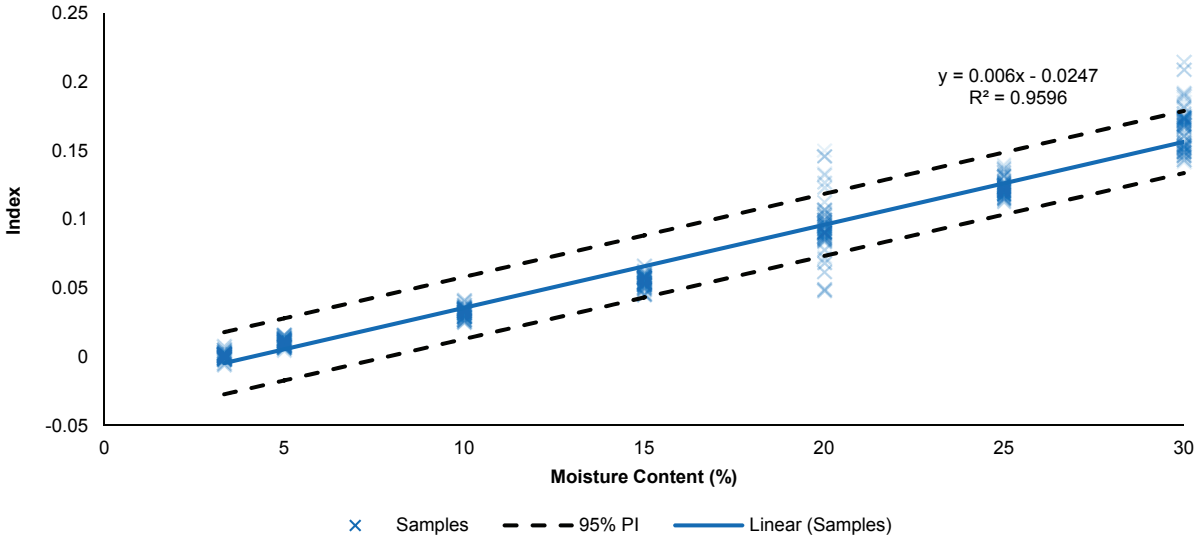

Figure 9. Normalized index for bare soil using 50 nm bands centered at 1300 nm and 1500 nm.

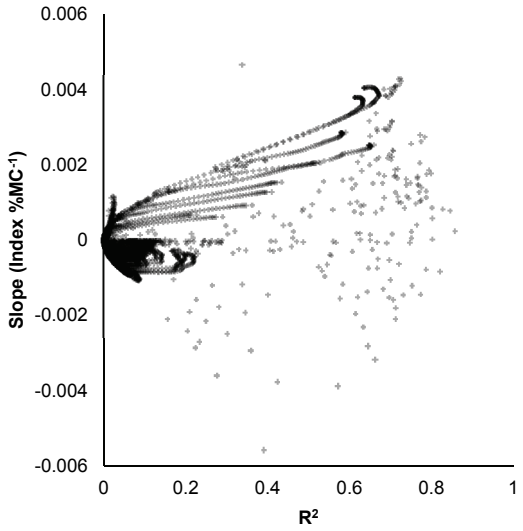

Figure 11. Slope of linear regression of reflectance and moisture content versus R^2 for wheat stalk residue.

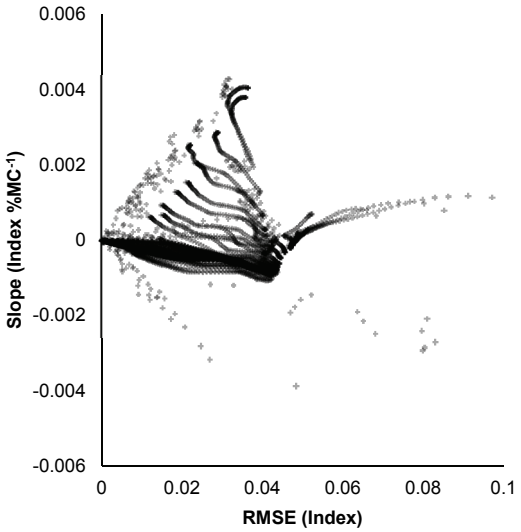

Figure 12. Slope of linear regression of reflectance and moisture content versus RMSE for wheat stalk residue.

tance between moisture contents was smaller. Again, the discontinuities could have been better addressed through a more complex calibration process, but that was deemed unnecessary for this experiment. The average reflectance was not well correlated with moisture content and was likely driven by the effective height of the stalk surface, which was less carefully controlled than the soil surface due to the physical structure of the stalks.

Because similar patterns between reflectance and wavelengths existed for both bare soil and wheat stalks, it was expected that the optimization process for stalks would provide a pair of "best" wavelengths close to the results for bare soil. Plots of R^2 (fig. 11) and RMSE (fig. 12) versus slope revealed similar patterns as wavelengths were incrementally changed, but the overall shapes differed from the results for bare soil. In both instances, optima occurred at smaller slopes and either lower R^2 or higher RMSE values, indicating that the index would not likely perform as well as it did for bare soil. However, the local optima still corresponded to the same pair of wavelengths near 1300 nm and 1500 nm, which indicated that the same sensor may function, albeit less accurately, in areas that include both bare soil and wheat stalk residue. A single pair of wavelengths across a variety of soil and crop material compositions would be advantageous for applying a low-cost sensor across varying commodities and production practices.

The index values from 50 nm wide bands centered at 1300 nm and 1500 nm for all samples are shown in figure 13 along with the linear regression model and 95% prediction interval. The variability in index calculation among samples at a given moisture content was large for all moisture contents, thus reducing the usefulness of the index for stalk moisture content. Two possible explanations for why the index failed to perform as well for stalks as it did for soil include: (1) the non-uniform

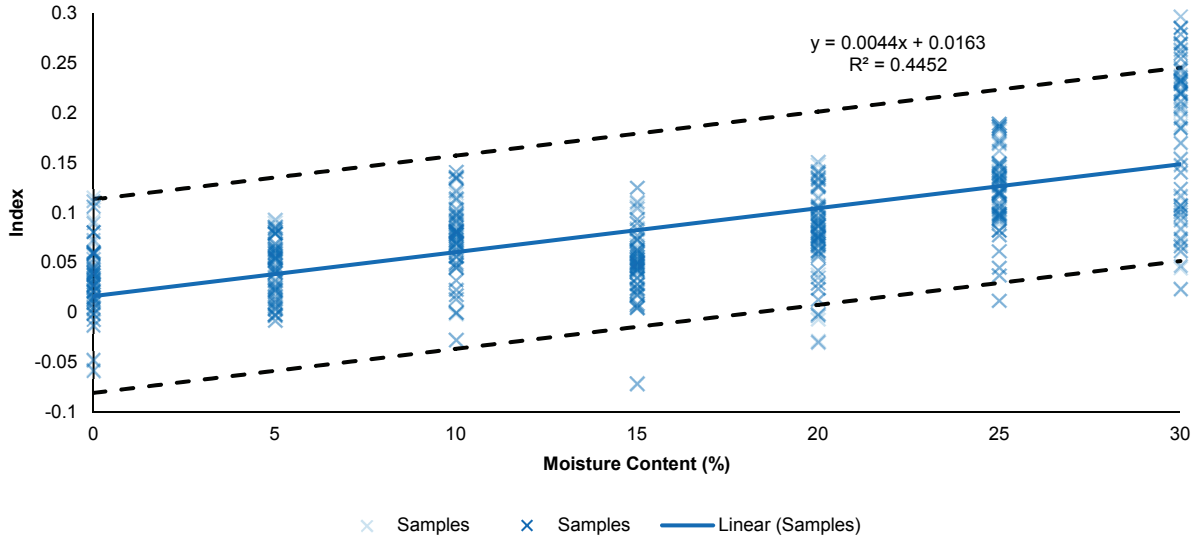

Figure 13. Normalized index for wheat stalk residue using 50 nm bands centered at 1300 nm and 1500 nm.

Table 2. Average index measurements for bare soil and wheat stalk residue at varying moisture contents and sensor heights.

Sample	Moisture Content (%)	Sensor Height H1	H2	H3	H4	H5
Bare soil	3.33	-0.0006	0.0016	0.0011	0.0027	0.0006
	5.0	0.0088	0.0111	0.0100	0.0122	0.0104
	10.0	0.0337	0.0335	0.0324	0.0316	0.0316
	15.0	0.0532	0.0581	0.0561	0.0557	0.0555
	20.0	0.0814	0.0936	0.0994	0.1001	0.1012
	25.0	0.1217	0.1230	0.1219	0.1253	0.1267
	30.0	0.1661	0.1716	0.1722	0.1615	0.1575
Wheat stalk residue	0.0	0.0101	0.0461	0.0201	0.0514	0.0497
	5.0	0.0236	0.0404	0.0487	0.0423	0.0574
	10.0	0.0105	0.0668	0.0784	0.0822	0.0939
	15.0	0.0422	0.0225	0.0551	0.0606	0.0599
	20.0	0.0457	0.0704	0.1021	0.0831	0.0863
	25.0	0.0705	0.0956	0.1330	0.1408	0.1362
	30.0	0.1908	0.1597	0.2056	0.2113	0.1835

Table 3. Parameter estimates and significance testing of height and moisture on the index.

Sample	Parameter	Estimate	Standard Error	t Ratio	Prob. > |t|
Bare soil	Height	0.0006356	0.000851	0.75	0.4604
	Moisture	0.0061931	0.000129	48.04	<0.0001
Wheat stalk residue	Height	0.0108258	0.003532	3.07	0.0044
	Moisture	0.0045207	0.000499	9.05	<0.0001

height of the stalks relative to the reflectance increased variability, and (2) the water absorbed by the stalks was not uniformly distributed, i.e., the moisture at the stalk surface did not necessarily represent the average moisture content.

SENSOR HEIGHT

Average index values for individual sensor heights and moisture contents are shown in table 2 for the bare soil and wheat stalk data. Results for bare soil showed a strong direct relationship between moisture content and the index value, while results for wheat stalk residue showed a weaker direct relationship. The sensor height above the sample was observed to influence the average reflectance, but the effect on the index calculation was not known. Therefore, a multifactor analysis of variance (ANOVA) ($\alpha = 0.05$) was used to determine if sensor height and moisture content significantly affected the index results (table 3). The ANOVA revealed that moisture content was significant while height was not for bare soil, and that both moisture and height were significant for wheat stalk residue. This result indicates the difficulty that low-cost field sensors may encounter when observing heterogeneous ground cover. Careful control of the sensor height, and perhaps classification of the ground cover, may be necessary for remotely sensing soil surface moisture content.

CONCLUSIONS

Moisture-controlled soil and wheat stalk residue samples were prepared and measured at varying heights using a reflectance probe connected to visible and near-infrared spectrometers. A computer program was written that used reflectance data to determine the optimal narrowband wavelengths when calculating NDWI based on user-defined constraints, and the statistical significance of sensor height and moisture content was determined for the "best" pair. Constraints for this study were configured to maximize the slope of the index (i.e., sensitivity to moisture) and either maximize the R^2 or minimize the RMSE of the index function. A linear model was chosen to represent the index when fitting parameters. Results showed that wavelengths centered near 1300 nm and 1500 nm, within the range of 400 to 1700 nm, produced the best index for individual samples. An advantage of this pair of wavelengths is that they can be sensed with a single type of sensor using narrowband optical filters. The 1500 nm band, when measured with an active ground-based sensor, will provide spectral information not available when using passive aerial or satellite-based remote sensing methods due to absorption from atmospheric moisture. When applied to all samples, the index performed well for the soil samples but poorly for the wheat stalk residue samples. Index calculations from soil reflectance measurements were highly linear ($R^2 > 0.95$) and exhibited small variability between samples at a given moisture content, regardless of measurement height. Index calculations from wheat stalk residue reflectance measurements were highly variable, which limited the usefulness of the index for this type of material. Based on these results, it is expected that crop residues, such as wheat stalks, will reduce the accuracy of remotely sensed soil surface moisture measurements. Future work should include heterogeneous samples that include both soil and crop residue in varying proportions to determine the composite response. As new low-cost sensors are developed, the optimization parameters used to determine the "best" wavelengths should be refined based on actual sensor response, rather than ideal assumptions.

ACKNOWLEDGEMENTS

This is Publication No. 17-05-083 of the Kentucky Agricultural Experiment Station and is published with the approval of the director. This work is supported in part by the USDA National Institute of Food and Agriculture, Multistate Project S1069. This work is supported in part by the National Science Foundation under Grant No. 1539070, Collaboration Leading Operational UAS Development for Meteorology and Atmospheric Physics (CLOUD-MAP), to Oklahoma State University in partnership with the University

of Oklahoma, the University of Nebraska-Lincoln, and the University of Kentucky. Special thanks to Jason Walton of the Department of Plant and Soil Sciences at the University of Kentucky for his help with preparing soil samples and collecting the wheat stalk residue used in this study.

REFERENCES

Benedetti, R., & Rossini, P. (1993). On the use of NDVI profiles as a tool for agricultural statistics: The case study of wheat yield estimate and forecast in Emilia Romagna. *Remote Sens. Environ., 45*(3), 311-326. http://dx.doi.org/10.1016/0034-4257(93)90113-C

Cardinale, B. J., Duffy, J. E., Gonzalez, A., Hooper, D. U., Perrings, C., Venail, P., ... Naeem, S. (2012). Biodiversity loss and its impact on humanity. *Nature, 486*(7401), 59-67. https://doi.org/10.1038/nature11148

Carlson, T. N., & Ripley, D. A. (1997). On the relation between NDVI, fractional vegetation cover, and leaf area index. *Remote Sens. Environ., 62*(3), 241-252. http://dx.doi.org/10.1016/S0034-4257(97)00104-1

Carlson, T. N., Dodd, J. K., Benjamin, S. G., & Cooper, J. N. (1981). Satellite estimation of the surface energy balance, moisture availability, and thermal inertia. *J. Appl. Meteorol., 20*(1), 67-87. https://doi.org/10.1175/1520-0450(1981)020<0067:seotse>2.0.co;2

Cassman, K. G. (1999). Ecological intensification of cereal production systems: Yield potential, soil quality, and precision agriculture. *Proc. Natl. Acad. Sci., 96*(11), 5952-5959. https://doi.org/10.1073/pnas.96.11.5952

Gao, B.-C. (1996). NDWI: A normalized difference water index for remote sensing of vegetation liquid water from space. *Remote Sens. Environ., 58*(3), 257-266. http://dx.doi.org/10.1016/S0034-4257(96)00067-3

Gu, Y. X., Brown, J. F., Verdin, J. P., & Wardlow, B. (2007). A five-year analysis of MODIS NDVI and NDWI for grassland drought assessment over the central Great Plains of the United States. *Geophys. Res. Lett., 34*(6), article L06407. https://doi.org/10.1029/2006GL029127

Hatfield, J. L. (2015). Environmental impact of water use in agriculture. *Agron. J., 107*(4), 1554-1556. https://doi.org/10.2134/agronj14.0064

Holland, K. H., Schepers, J. S., Shanahan, J. F., & Horst, G. L. (2004). Plant canopy sensor with modulated polychromatic light source. *Proc. 7th Intl. Conf. on Precision Agriculture and Other Precision Resources Management* (pp. 148-160). St. Paul, MN: University of Minnesota, Precision Agriculture Center.

Huang, J., Chen, D., & Cosh, M. H. (2009). Sub-pixel reflectance unmixing in estimating vegetation water content and dry biomass of corn and soybeans cropland using normalized difference water index (NDWI) from satellites. *Intl. J. Remote Sens., 30*(8), 2075-2104. https://doi.org/10.1080/01431160802549245

Huete, A. R. (1988). A soil-adjusted vegetation index (SAVI). *Remote Sens. Environ., 25*(3), 295-309. http://dx.doi.org/10.1016/0034-4257(88)90106-X

Mullen, R. W., Freeman, K. W., Raun, W. R., Johnson, G. V., Stone, M. L., & Solie, J. B. (2003). Identifying an in-season response index and the potential to increase wheat yield with nitrogen. *Agron. J., 95*(2), 347-351. https://doi.org/10.2134/agronj2003.3470

Nemani, R. R., & Running, S. W. (1989). Estimation of regional surface resistance to evapotranspiration from NDVI and thermal-IR AVHRR data. *J. Appl. Meteorol., 28*(4), 276-284. https://doi.org/10.1175/1520-0450(1989)028<0276:eorsrt>2.0.co;2

Penuelas, J., Pinol, J., Ogaya, R., & Filella, I. (1997). Estimation of plant water concentration by the reflectance water index WI (R900/R970). *Intl. J. Remote Sens., 18*(13), 2869-2875. https://doi.org/10.1080/014311697217396

Raun, W. R., Solie, J. B., Johnson, G. V., Stone, M. L., Mullen, R. W., Freeman, K. W., ... Lukina, E. V. (2002). Improving nitrogen use efficiency in cereal grain production with optical sensing and variable rate application. *Agron. J., 94*(4), 815-820. https://doi.org/10.2134/agronj2002.8150

Solari, F., Shanahan, J., Ferguson, R., Schepers, J., & Gitelson, A. (2008). Active sensor reflectance measurements of corn nitrogen status and yield potential. *Agron. J., 100*(3), 571-579. https://doi.org/10.2134/agronj2007.0244

Svensgaard, J., Roitsch, T., & Christensen, S. (2014). Development of a mobile multispectral imaging platform for precise field phenotyping. *Agron., 4*(3), 322. https://doi.org/10.3390/agronomy4030322

USDA. (2015). Irrigation and water use. Washington, DC: USDA. Retrieved from https://www.ers.usda.gov/topics/farm-practices-management/irrigation-water-use/

Yule, I. J., Hedley, C. B., & Bradbury, S. (2008). Variable-rate irrigation. *Proc. 12th Annual Symp. on Precision Agriculture Research & Application in Australasia* (pp. 24-26). Sydney, Australia: University of Sydney, Australian Centre for Precision Agriculture. Retrieved from http://sydney.edu.au/agriculture/pal/documents/Symposium_2008.pdf